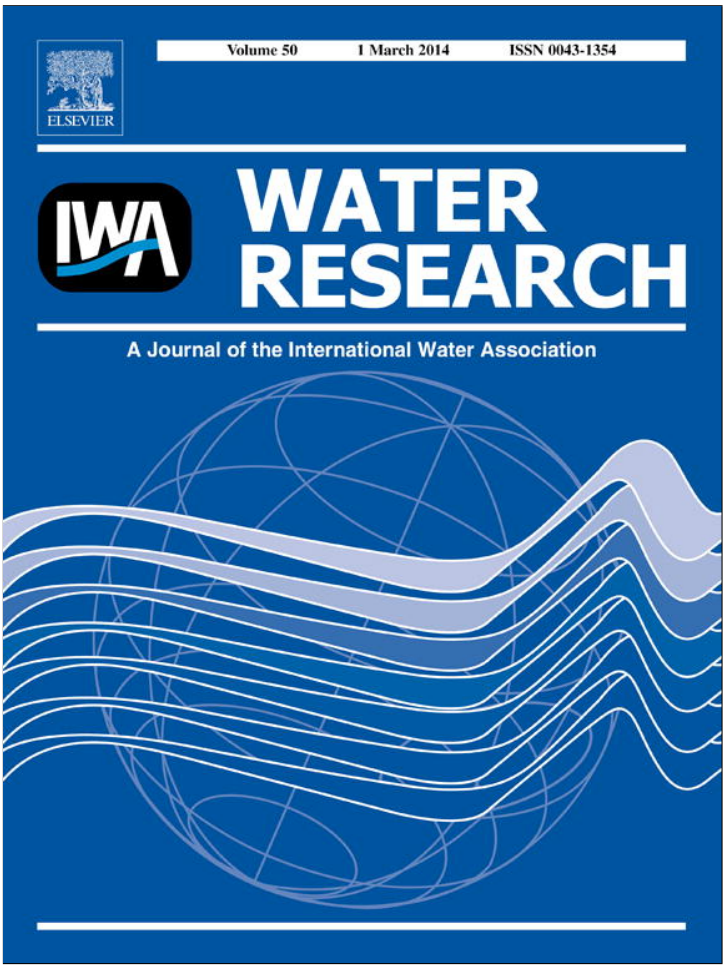

WATER RESEARCH 50 (2014) 189–199

Available online at www.sciencedirect.com

ScienceDirect

journal homepage: www.elsevier.com/locate/watres

Combination of ozonation and photocatalysis for purification of aqueous effluents containing formic acid as probe pollutant and bromide ion

F. Parrino [a], G. Camera-Roda [b], V. Loddo [a,*], G. Palmisano [a], V. Augugliaro [a]

[a] Dipartimento di Energia, Ingegneria dell'Informazione e Modelli Matematici (DEIM), University of Palermo, Viale delle Scienze Ed. 6, Palermo 90128, Italy

[b] Department of Civil, Chemical, Environmental, and Materials Engineering, University of Bologna, via Terracini 28, Bologna 40131, Italy

ARTICLE INFO

Article history:
Received 6 August 2013
Received in revised form
29 November 2013
Accepted 3 December 2013
Available online 13 December 2013

Keywords:
Ozonation
Photocatalysis
Bromate
Water purification
Photocatalytic ozonation
Advanced oxidation processes

ABSTRACT

The treatment by advanced oxidation processes (AOPs) of waters contaminated by organic pollutants and containing also innocuous bromide ions may generate bromate ions as a co-product. In the present work heterogeneous photocatalysis and ozonation have individually been applied and in combination (integrated process) to degrade the organic compounds in water containing also bromide anions. The results show that: i) the sole photocatalysis does not produce bromate ions and in the case of its presence, it is able to reduce bromate to innocuous bromide ions; ii) the integration of photocatalysis and ozonation synergistically enhances the oxidation capabilities; and iii) in the integrated process bromate ions are not produced as long as some oxidizable organics are present.

1. Introduction

Water detoxification can provide a substantial contribution to water conservation, which is one of the primary objectives of sustainability. In fact, organic polluted and contaminated waters can be recovered and utilized (or reutilized in a closed system) with vital savings of water resources. Some Advanced Oxidation Processes (AOPs), such as ozonation and photocatalysis, have been demonstrated to be able to accomplish this task (Hoignè, 1998; Beltran, 2003; Chong et al., 2010; Pichat, 2013; Augustina et al., 2005) and to get rid of the organics which are recalcitrant to biological degradation. Therefore, research on these technologies is continuously growing in the recent years. However, the possible formation of undesired oxidation by-products must be taken into account since they may negatively affect the quality of the water. For instance, it is known that bromide ions can be oxidized to bromate ions, which are of major concern for human health (WHO, 1993) and aquatic life (Hutchinson et al.,

* *Corresponding author*. Tel.: +39 (0) 91 238 63722.
E-mail addresses: francesco.parrino@unipa.it (F. Parrino), giovanni.cameraroda@unibo.it (G. Camera-Roda), vittorio.loddo@unipa.it (V. Loddo), giovanni.palmisano@unipa.it (G. Palmisano), vincenzo.augugliaro@unipa.it (V. Augugliaro).

0043-1354/$ – see front matter © 2013 Elsevier Ltd. All rights reserved.
http://dx.doi.org/10.1016/j.watres.2013.12.001

1997; Buttler et al., 2005). On the other hand, bromide ions are almost always present in aqueous systems albeit at various concentrations. Indeed, the Br^- concentrations are relatively low in rainwater, ranging from 0 to 110 μg L^{-1} (Neal et al., 2007), but may increase in groundwater where the normal values are between 10 and 2 × 10^3 μg L^{-1} (Flury and Papritz, 1993), to reach a much higher content in seawater (typically about 67 × 10^3 μg L^{-1}). Areas close to the sea usually show larger Br^- contents in water and soils than inland areas (Yuita, 1983). The three major manmade releases of bromine into the environment are from mining, from emission of 1,2-dibromoethane, which is used as scavenger in leaded fuel (Kittel, 1983), and from the use of fertilizers and pesticides in agriculture (Bowen, 1979) causing a considerable increase of concentration.

Furthermore, bromide is found in nearly every drinking water source at concentrations ranging from less than 10 to nearly 3 × 10^3 μg L^{-1} (Krasner et al., 1989). In a study on the drinking water sources in USA, Amy et al. (1994) reported an average bromide level ranging between 80 and 100 μg L^{-1}.

The choice of the AOP for treating wastewater containing bromide is very critical; ozonation of natural waters in the presence of organic compounds and significant bromide levels can cause the harmful formation of brominated organics (Cavanagh et al., 1992; Richardson et al., 1999) and bromate ions (Siddiqui et al., 1995). Since the 90s, the International Agency for the Research on Cancer (IARC) has classified bromate as a potentially carcinogenic species. The WHO (1993) guidelines calculated that a concentration of bromate of 3 μg L^{-1} is associated with an upper-bound excess lifetime cancer risk of 10^{-5}. However, due to limitations in available analytical and treatment methods, WHO recommended a provisional guideline value of 25 μg L^{-1}, for which the risk increases to 7 × 10^{-5}. The United States Environmental Protection Agency (USEPA) adopted a minimal lethal concentration (MLC) for bromate of 10 μg L^{-1} based on the considerations about the minimal health risk, the current available treatment technologies, and the limits of experimental analysis. The same value was proposed by the Drinking Water Commission of the European Union (Council Directive 98/93/EC, 1998). Therefore, these limitations must be considered in any kind of proposed water treatment and guidelines must be drawn to avoid or to control the increase of bromate, which accumulation can be harmful in particular in closed, recirculation systems.

Ozonation (see e.g. Von Gunten, 2003) and photocatalysis (see e.g. Ravelli et al., 2009) are promising AOPs for water treatment. During ozonation of water containing bromide, the formation of bromate occurs. In particular, oxidation by ozone and by the induced oxidizing agents (e.g., the hydroxyl radical, $^{\bullet}OH$) results in the formation of different intermediate brominated species (hypobromous acid, hypobromite ions, bromite, bromide radicals, and hypobromite radicals) and eventually bromate (BrO_3^-) (Siddiqui et al., 1995).

Heterogeneous photocatalysis is one of the most studied AOPs in the last two decades (Herrmann, 2005; Augugliaro et al., 2010; Akpan and Hameed, 2011a, 2011b; Ibhadon and Fitzpatrick, 2013; Pichat, 2013). This catalytic process uses semiconductor oxides irradiated by UV light in presence of oxygen at room temperature. The light activates the photocatalyst and generates on its surface electron–hole pairs, which cause the occurrence of redox reactions of the adsorbed species. This method has been successfully used for wastewater treatment and it is suitable to perform the complete degradation of organic and inorganic pollutants, the reduction of metal ions and the inactivation of many bacteria (Augugliaro et al., 2004; Akpan and Hameed, 2010; Ali et al., 2011; Sunada et al., 2003). Heterogeneous photocatalysis has been also used for purification of indoor air and gaseous effluents contaminated by organics (Pichat et al., 2000; Taranto et al., 2007).

Ozone in combination with heterogeneous photocatalysis, also called "photocatalytic ozonation" (Tanaka et al., 1996; Klare et al., 1999; Piera et al., 2000), has been studied in liquid phase to treat aniline (Sanchez et al., 1998), phenol (Villaseñor et al., 2002), formic acid (Wang et al., 2002), cyanide ions (Hernandez-Alonso et al., 2002), oxalic acid (Addamo et al., 2005) and monochloroacetic acid (Mas et al., 2005). In this "integrated process" a significant improvement of the oxidation performances has been reported since the rate of mineralization of organic substances is greatly enhanced. Likely explanation of the onset of this effect (Tanaka et al., 1996; Klare et al., 1999; Piera et al., 2000; Sanchez et al., 1998) is that ozone is able to generate $^{\bullet}OH$ radicals on the TiO_2 surface through the formation of an $O_3^{\bullet-}$ ozonide radical ion. Therefore, the production of $^{\bullet}OH$ radicals on the irradiated surface of photocatalyst would be more effective in the presence of ozone than with oxygen.

In the present work heterogeneous photocatalysis and ozonation have been applied individually or in combination (integrated process) to degrade the organic compounds in water containing bromide anions. Particular attention has been given to the strategies that allow a control of the formation of bromate. In order to represent the organics which are present in wastewaters, formate ions and/or formic acid were adopted since they are small molecules whose degradation pathway is simple so that a more direct analysis is possible of the fundamental phenomena which take place in the system. 4-nitrophenol was also utilized in selected runs as probe molecule to check the effect of the chemical nature of the contaminant on the oxidation process. Photocatalysis, ozonation and the integrated process were studied in order to determine the kinetics of: i) degradation of the organic compound in the presence of bromide ions and ii) formation of bromate ions.

2. Material and methods

The reactions were carried out in an annular batch photoreactor with Pyrex walls which do not absorb UV-A light. The set up of the reacting system is schematically shown in Fig. 1. The 500 cm^3 photoreactor was equipped with ports in the upper part in order to feed gases, to measure pH and temperature and to withdraw samples of the reacting suspension. A medium pressure Hg lamp (Helios Italquartz, Italy, nominal power 125 W) was positioned on the axis of the photoreactor. The lamp was cooled by a Pyrex water-cooling thimble constituting the inner part of the annulus. The emission spectrum of the lamp presents a maximum at 365 nm. The

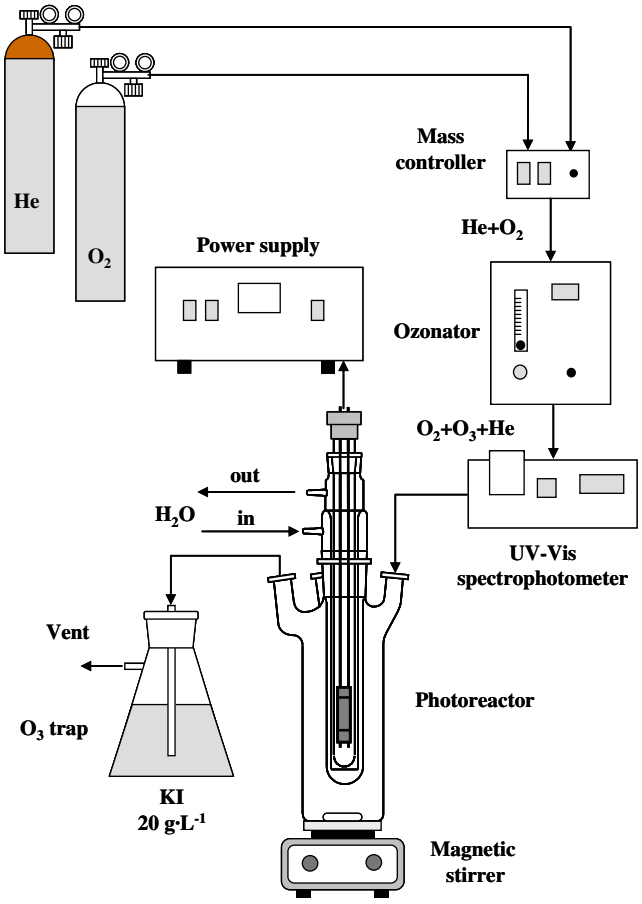

Fig. 1 – Scheme of the reacting system.

photon flux was measured by a radiometer (Delta Ohm DO 9721) with an irradiance probe LP9021 UVA (315–400 nm) at different heights on the outer wall of the reactor. The measured average value was 7 mW cm^{-2} in the absence of the photocatalyst.

Both the initial concentrations of formate and bromide ions and the flow rate of the gas bubbled into the suspension were varied in the experiments. Some runs were carried out also with the initial presence of bromate ion with or without formate ion. In a few runs another aromatic compound, 4-nitrophenol (4-NP), was used to substitute formate ion in order to check the influence, if any, of the chemical nature of the substrate on the behaviour of the processes. Pure oxygen or ozone–oxygen mixtures with two different compositions were continuously bubbled into the liquid phase during the runs at a constant flow rate of 300 cm^3 min^{-1}. The measured concentration of the dissolved oxygen in the liquid phase was 1.3×10^{-3} M in the case of pure oxygen and 2.6×10^{-4} M when a mixture of He–O_2 (80%–20%) was bubbled in the solution. Nitrogen was not used for dilution since it was found that, when air was used for ozone production, nitrogen was finally oxidised to nitrate. Ozone was produced by feeding pure O_2 or the He–O_2 mixture to the ozonator (Microlab), obtaining in this way ozone concentrations of 4.9×10^{-4} and 0.55×10^{-4} M, respectively. Adopting the Henry's constants (Lide, 1994), the ozone concentrations were 1.05×10^{-4} M (pure O_2) and 0.58×10^{-4} M (He–O_2 mixture), while the O_2 concentrations were 1.2×10^{-3} M (pure O_2) and 2.5×10^{-4} M (He–O_2 mixture). The initial formate concentrations were: 0.2, 0.5, 1, and 2 mM. The initial bromide concentrations ranged between 0.1 and 1 mM. For the runs carried out starting with bromate anions, its initial concentration was 0.5 mM. All the chemicals were reagent grade (Sigma–Aldrich) and de-ionized water was used for the preparation of the solutions. Generally the pH was not adjusted, so that the measured pH values were between 6 and 7.5 for initial formate concentrations ranging from 0.2 to 2 mM. For initial formic acid concentrations of 0.1 and 1 mM the measured pH values were 3.4 and 3.6, respectively. Using 0.15 mM 4-NP solution, the measured pH was 5.7. The temperature was 300 K.

TiO_2 Degussa Aeroxide P25 (ca. 80% anatase and 20% rutile, BET specific surface area: 50 m^2 g^{-1}) was used without any preliminary treatment. Before any run weighed amount of this photocatalytic powder was dispersed in a given volume of the solution. For most of the runs the amount of photocatalyst was 0.2 g L^{-1}; this amount of catalyst is sufficient to absorb in the reactor almost all the photons emitted by the lamp. The photoreactivity runs lasted from 1 to 10 h. Before turning on the lamp, the system was maintained in the dark for 30 min in order to reach stable conditions. Samples of the reacting solution (3 cm^3) were withdrawn at fixed intervals of time from the reactor. The samples were immediately filtered by means of a PTFE filter (Millipore) with pore diameter of 0.2 μm to remove the photocatalyst and then the concentration of ions was measured by ion exchange chromatography (Dionex DX 120) equipped with an Ion Pac AS14 4 mm column (250 mm long, Dionex). Aqueous solutions of $NaHCO_3$ (8 mM) and Na_2CO_3 (3.5 mM) were used as eluents at a flow rate of 1.67×10^{-2} cm^3 s^{-1}. In order to determine the concentration of ozone in the gas phase bubbled into the reacting system, the absorbance of gaseous ozone was measured at 254 nm by using a UV–Vis spectrophotometer (Shimadzu). A preliminary calibration was performed by bubbling the O_2–O_3 mixture in KI aqueous solution and measuring the quantity of iodide anion oxidized by the ozone to iodate. The residual ozone contained in the gaseous stream leaving the reactor was abated in a trap containing an aqueous solution of KI.

3. Results and discussion

3.1. *Homogeneous system*

Preliminary runs, carried out in the absence of catalyst, indicated that the concentration of formate and/or bromide ions remained constant during the bubbling of oxygen in the solution and/or during the UV-A irradiation. The presence of ozone in the reacting solution led to a decrease in the concentration of formate and bromide and the extent of this decrease is not affected by irradiation with UV-A light.

As it is well known, the ozone dissolved in water is unstable. The decay of ozone in water is characterized by a fast initial rate, followed by a second phase in which ozone decreases with first-order kinetics (Von Gunten, 2003). The mechanism and the kinetics of the elementary reactions involved in ozone decomposition have been deeply

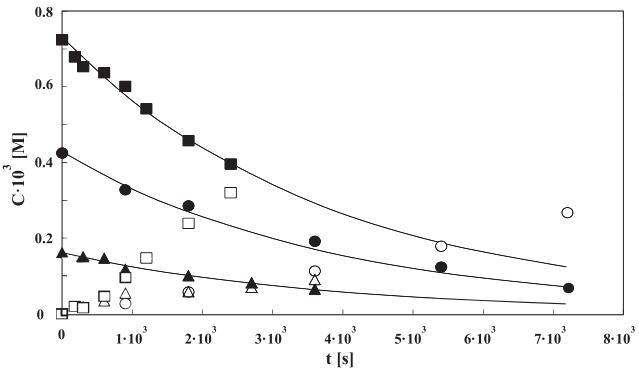

Fig. 2 – Experimental values of bromide (full symbols) and bromate (empty symbols of the corresponding bromide symbol) ions concentration vs. reaction time for runs carried out in the contemporary presence of O_3 and oxygen. Ozone concentration in the liquid phase: 1.05×10^{-4} M.

investigated (Forni et al., 1982; Staehelin and Hoigné, 1982, 1985). The major secondary oxidant formed by ozone decomposition in water is the hydroxyl radical. The stability of ozone largely depends on the pH as hydroxyl radicals initiate ozone decomposition.

Dissolved ozone causes the oxidization of bromide ion to bromate ion. Fig. 2 shows the experimental results of representative runs carried out at different initial concentration of bromide and at the highest concentration of ozone in the liquid phase (1.05×10^{-4} M).

The oxidation rate of bromide is hypothesised to obey the following kinetic law:

$$-\frac{dC_{Br^-}}{dt} = k_2 C_{Oz}^{\alpha} C_{Br^-}^{\beta} = k_2' C_{Br^-}^{\beta} \quad (1)$$

in which the subscripts Br⁻ and Oz refers to bromide and ozone, respectively, C indicates the concentration, t the time and k_2 is the second order kinetic constant. $k_2 C_{Oz}^{\alpha}$ may be substituted with k_2' since ozone was continuously bubbled during the reaction and thus its concentration in liquid phase is constant during the experimental runs. By adopting different values of β in the integrated form of eq. (1), it has been found that the best fit is obtained for $\beta = 1$, i.e. the bromide degradation is first order with respect to bromide concentration, in fact the exponential decay of the bromide concentration reported in Fig. 2 fits very satisfactorily the experimental data.

The bromide oxidation rate is first order also with respect to ozone as shown in Fig. 3 where the k_2' values, obtained by experimental runs carried out at different ozone concentrations but constant bromide (0.5×10^{-3} M), are plotted against the ozone concentrations in the liquid phase. The slope of the fitted straight line is 2.4 M^{-1} s^{-1} which represents the value of k_2. This value is lower than the one found in the literature (Haag and Hoigne, 1983) but it must be noted that the ozone concentrations used in this work are much higher than those utilized by Haag and Hoigné.

It is reported (Song et al., 1996) that in ozonated water containing bromide ion the major bromate formation is via three main pathways: (i) direct ozonation; (ii) direct-indirect ozonation; and (iii) indirect-direct ozonation. It is known that the previous pathways are strongly affected by ozone and bromide concentration and pH (Siddiqui et al., 1995). However, as the value of pH used in the present investigation was less than 7.5, it has been assumed that bromate formation mainly occurs through the direct ozonation pathway (Gillogly et al., 2001).

Dissolved ozone is able to oxidize formate ion and formic acid as shown in Fig. 4. As for the case of bromide, the experimental results are fitted very well by a first order kinetics with respect to both formate and formic acid. The values of the kinetic constant obtained by a least squares best fitting procedure are 2.36 and 2.05 M^{-1} s^{-1} for the formate and the formic acid, respectively. These values differ from 100 M^{-1} s^{-1} obtained by Hoigné and Bader (1983) but are quite closely agreeing with k value of 1.53 M^{-1} s^{-1} reported by Yapsakli and Can (2004). The discrepancy may come from the type of hydroxyl radical scavengers used (Hoigné and Bader utilized n-propanol), or from differences in ozone concentrations.

The direct oxidation of formate anion is an electrophilic addition that leads to an intermediate adduct generated by

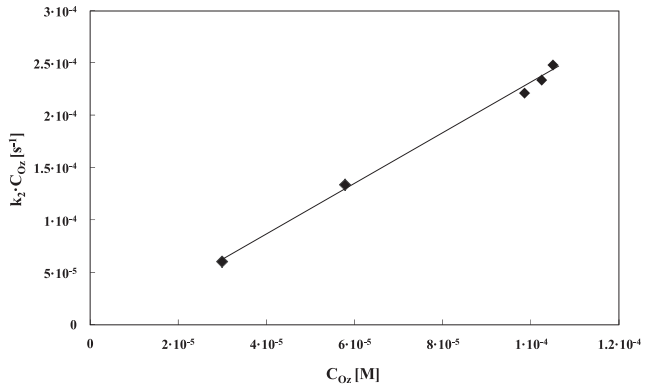

Fig. 3 – Values of pseudo-first order rate constant of bromide vs. the ozone concentration in liquid phase. Initial bromide concentration equal to 0.5×10^{-3} M.

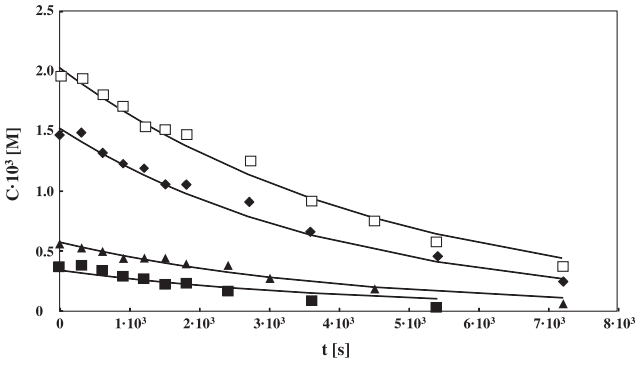

Fig. 4 – Concentrations of formate ion (full symbol) and formic acid (empty symbol) vs. reaction time for runs carried out in presence of both O_3 and oxygen. Ozone concentration in the liquid phase: 1.05×10^{-4} M.

ozone insertion followed by formation of CO_2, molecular oxygen and hydroxide ions (Yapsakli and Can, 2004):

3.1.1. *Direct ozonation*

$$HCOO^- + O_3 \rightarrow CO_2 + O_2 + {}^-OH \quad (2)$$

Formate anions can also react with •OH radicals according to the following reaction:

3.1.2. *Indirect ozonation*

$$HCOO^- + 2{}^\bullet OH \rightarrow CO_2 + H_2O + {}^-OH \quad (3)$$

In all the runs the pH increased slightly during the reaction and it remained between 3.7 and 5.4 with formic acid, or between 6.7 and 7.7 using formate ions. At these pH conditions the formate oxidation proceeds mainly via direct ozonation (Eq. (2)).

Fig. 5 shows the time evolution of formate concentrations for runs in the presence of bromide ions and UV-A radiation and with a concentration of dissolved ozone of 1.05×10^{-4} M. Runs carried out under dark conditions are also reported in Fig. 5 for the sake of comparison.

The linearity of data reported in Fig. 5 shows that the formate oxidation kinetics is zero order. The results obtained in the runs in the presence of UV-A radiation indicate that the light does not affect the homogeneous degradation rate of formate ions by ozone. The runs at various concentration of dissolved ozone showed that the reaction kinetics is first order with respect to ozone (experimental data not shown).

On the basis of these observations the kinetics of formate oxidation in the presence of dissolved ozone can be expressed by the following equation:

$$-\frac{dC_F}{dt} = k_F \cdot C_F^0 \cdot C_{Oz}^1 \quad (4)$$

in which C_F is the formate concentration. The value of the first order rate constant, k_F, is 4.26×10^{-3} s^{-1}.

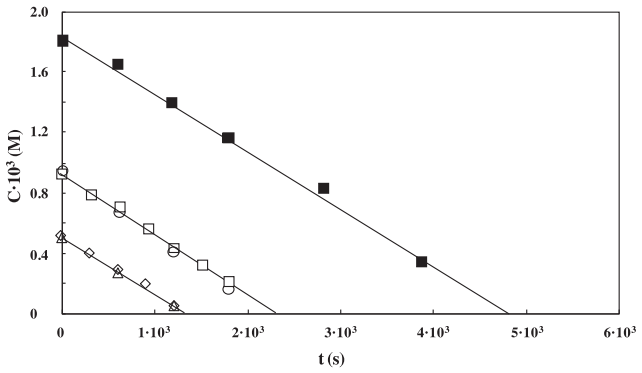

Fig. 5 – Experimental values of formate ion concentration in the presence of 0.45 mM Br^-, vs. reaction time for runs carried out in the simultaneous presence of O_3 and oxygen. Ozone concentration in the liquid phase: 1.05×10^{-4} M (runs identified by Δ and ○ were carried out in dark conditions).

Once the kinetics of the ozone induced oxidation of bromide and of formate has been established, it is important to assess if it changes when these two compounds are simultaneously present. Fig. 6 reports the concentrations of the relevant chemical species in this case. It can be observed that bromide does not react as long as formate is present in solution. Only after that formate is almost completely oxidized, bromate formation occurs. It should be noted that the produced bromate ions do not exactly equal the disappeared bromide ions, probably due to the formation of small amounts of intermediate brominated species.

3.2. *Heterogeneous system*

The photocatalytic oxidation of formate ions was carried out by using the same apparatus used for the experiments in homogeneous phase. A preliminary study was performed in order to determine a suitable amount of photocatalyst. Different catalyst amounts were used in the presence of 1 mM formate. Fig. 7 shows the optimum amount of photocatalyst for the oxidation of formate. It can be noticed that the initial reaction rate increases with the catalyst amount up to a value of ca. 0.2 g L^{-1} and at higher amounts it remains almost constant. This is the usual trend in photocatalytic reactions (Muneer et al., 2005). On the basis of these results the value of 0.2 g L^{-1} was chosen as an appropriate photocatalyst amount for all the other experiments.

Fig. 8 shows the results of photocatalytic runs carried out at different formate ion concentrations and with the continuous bubbling of oxygen. Fig. 8 also reports the formate concentration values obtained in a run in the presence of 0.5 mM of bromide ion. It is worth noting that bromide ions do not affect the photocatalytic oxidation of formate.

Fig. 9 shows that, during the photocatalytic degradation of formate ion, the concentration of bromide does not change indicating that bromide ions do neither react in a photocatalytic system nor they participate in redox reactions, hence their concentrations are not altered in the liquid phase.

Bromide ion can react with the hydroxyl radical generated during photocatalysis according to the following equations:

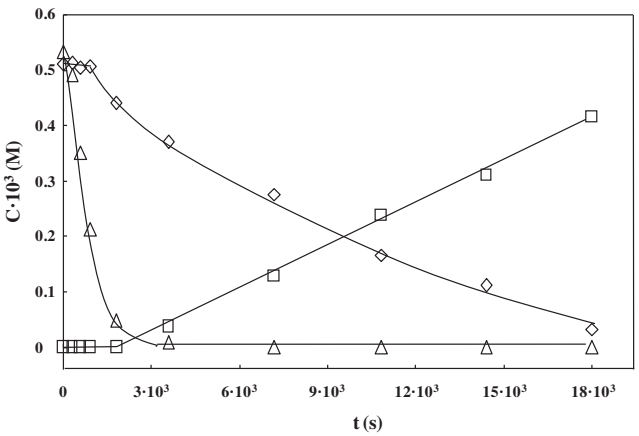

Fig. 6 – Formate (Δ), bromide (◇) and bromate (□) concentrations versus time for a run carried out in homogeneous phase in the presence of an ozone concentration in aqueous solution of 1.05×10^{-4} M.

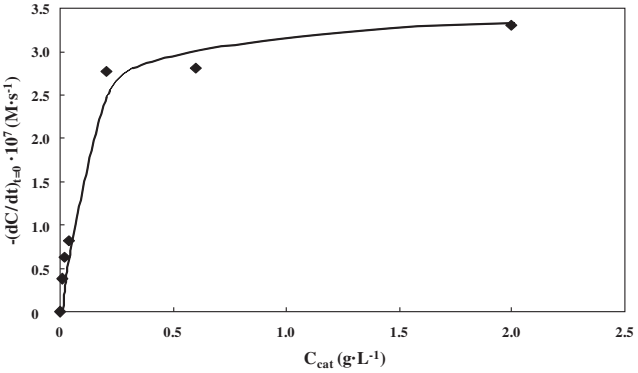

Fig. 7 – Optimum amount of photocatalyst for the oxidation of formate employing formate initial concentration of 1 mM.

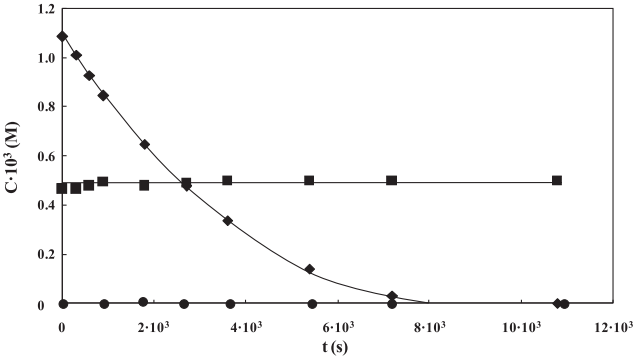

Fig. 9 – Experimental values of formate (◆), bromide (■) and bromate (●) ion concentration vs. reaction time for a run with simultaneous presence of TiO_2, oxygen and UV-A irradiation.

$$Br^- + {}^\bullet OH \rightarrow Br^\bullet + OH^- \quad (5)$$

$$Br^\bullet + {}^\bullet OH \rightarrow HOBr \quad (6)$$

$$HOBr \rightarrow OBr^- + H^+ \quad (7)$$

Then, hypobromite ion species can be reduced by the electrons generated onto the photocatalyst's surface:

$$OBr^- + 2e^- + H_2O \rightarrow Br^- + 2OH^- \quad (8)$$

Therefore, these pathways finally lead to the recovery of bromide ion. Alternatively, another pathway leads to the reduction of hypobromous acid to bromide. In fact, in the pH range (6–8) used in this study, HOBr generated according to Eq. (6), is mostly present in its protonated form and H_2O_2, which can be formed during the photocatalytic process, can act as a scavenger by transforming hypobromite into bromide (Von Gunten and Pinkernell, 2000).

In parallel, the oxidation of formate ions with photocatalysis is mediated by the oxidant species produced on the surface of the irradiated catalyst according to the following chemical equation:

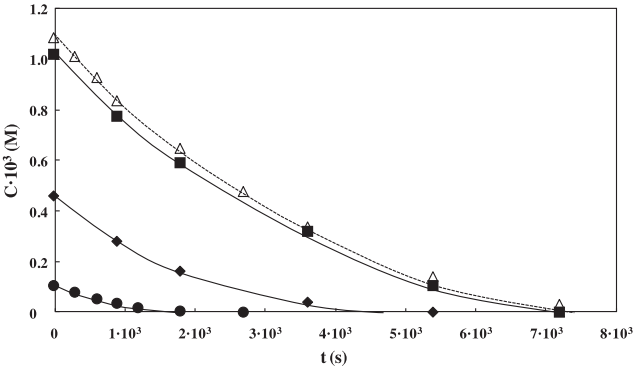

Fig. 8 – Experimental values of formate ion concentration vs. reaction time for runs carried out with the simultaneous presence of TiO_2, oxygen and UV-A irradiation. With (empty symbols) and without (full symbols) bromide ion.

$$HCOO^- + 2{}^\bullet OH \rightarrow CO_2 + OH^- + H_2O \quad (9)$$

By considering that formate anion and oxygen can be adsorbed on different types of sites existing on the irradiated catalyst surface (Augugliaro et al., 2008), the kinetics of formate oxidation depends on the coverage by oxygen and formate anion. On these grounds, a second-order surface reaction rate can be written in terms of Langmuir–Hinshelwood model as:

$$r_{S-F} \equiv -\frac{1}{S_A}\frac{dN_F}{dt} = -\frac{V}{S_A}\frac{dC_F}{dt} = k''_{Ox}\theta_{Ox}\theta_F \quad (10)$$

where r_{S-F} represents the formate moles reacted per unit time and surface area, k''_{Ox} is the surface second-order rate constant, and θ_{Ox} and θ_F are the fractional sites coverage by oxygen and formate anion, respectively, adsorbed on irradiated TiO_2 surface and S_A is the BET surface area. The θ_{Ox} and θ_F fractions are related to oxygen and formate concentration in the aqueous phase by the Langmuir isotherm:

$$\theta_{Ox} = \frac{K_{Ox}C_{Ox}}{1 + K_{Ox}C_{Ox}}; \quad \theta_F = \frac{K_F C_F}{1 + K_F C_F} \quad (11)$$

in which K_{Ox} and K_F are the equilibrium adsorption constants, and C_{Ox} and C_F the concentrations of oxygen and formate anion, respectively. As all the experiments were performed in a batch reactor with a continuous bubbling of oxygen, it can be assumed for all the runs that the θ_{Ox} term is constant.

By substituting Eq. (11) into Eq. (10) and integrating with the initial condition that $C_F = C_F^0$ at $t = 0$, the following relationship between t and C_F is obtained:

$$t = \frac{1}{k'_{Ox}\frac{S}{V}K_F}\ln\frac{C_F^0}{C_F} + \frac{1}{k'_{Ox}\frac{S}{V}}(C_F^0 - C_F) \quad (12)$$

where $k'_{Ox} = k''_{Ox}\theta_{Ox}$ is the surface pseudo-first order rate constant.

By applying a least-squares best fitting procedure to the photoreactivity data obtained from all the experiments, it has been determined that the values of K_F and k'_{Ox} are 100 M^{-1} and 2.25 × 10^{-8} mol m^{-2} s^{-1}, respectively. The satisfactory fitting of the model to the experimental data is observed in Fig. 10 where the model results given by Eq. (12) are compared with the experimental data. Note that the value of k'_{Ox} depends on

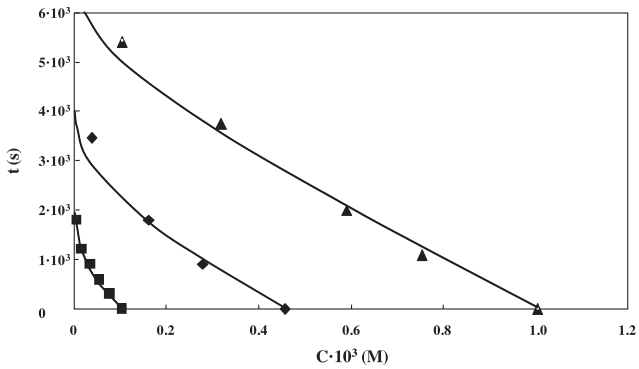

Fig. 10 – Comparison between the experimental data (full symbols) and the Langmuir–Hinshelwood model (continuous lines) of selected runs.

the dissolved oxygen concentration according to the following relationship:

$$k'_{Ox} = k''_{Ox} \cdot \theta_{Ox} = k''_{Ox} \cdot \frac{K_{Ox} \cdot C_{Ox}}{1 + K_{Ox} \cdot C_{Ox}} \quad (13)$$

Selected runs carried out at different oxygen concentrations in solution allowed to determine by a best fitting procedure with the least squares method, the values of k''_{Ox} and K_{Ox}, which are reported in Table 1.

The photocatalytic experiments carried out in the presence of bromate ions indicate that bromate is almost stoichiometrically reduced to bromide ion. This finding is in agreement with literature (Brookman et al., 2011). Fig. 11 shows a selected experiment with an initial bromate concentration of 0.5 mM.

Therefore, two indications of practical relevance for the control of bromate formation are obtained from the photocatalytic experiments: i) the photocatalytic treatment of contaminated water containing bromide ions does not generate bromate ions; ii) even in the case that bromate ions are present in the contaminated water, photocatalysis is capable to transform them into innocuous bromide ions.

The analysis was completed by integrating ozonation and photocatalysis. In preliminary runs carried out with formate and bromide ions in the presence of TiO_2 and ozone, without irradiating the system, it was observed that the decrease of the formate and bromide concentrations is almost the same obtained in the homogeneous ozonation (without TiO_2) thus indicating that the possible catalytic reaction on the TiO_2 surface plays a negligible role (Nawrocki and Kasprzyk-Hordern, 2010) at least for liquid phase systems. Indeed, for gas phase systems the presence of TiO_2 enhances ozone decomposition rate thus improving the organic oxidation (Ohtani et al., 1992; Pichat et al., 2000).

Other preliminary experiments with photocatalysis coupled with ozonation were then carried out in presence of formate and bromide at different TiO_2 concentrations in order to determine the suitable catalyst amount. The formate oxidation rates showed the same behaviour observed without ozonation (see Fig. 8) so that the same value of 0.2 g L^{-1} was adopted also for the integrated process.

It was observed that also in the integrated process the formate oxidation is not affected by the presence of bromide ion and the bromide oxidation to bromate occurs only after the disappearance of formate ions. A similar behaviour was observed by Mas (Mas et al., 2005) in the presence of Cl^- ions, which are oxidised to ClO_3^- only when the system does not contain organic compounds any longer. These behaviours are apparent in Fig. 12 which shows the results obtained with the integrated process for a selected run carried out with formate and bromide ions.

In the integrated process, the formate oxidation occurs through three routes: (i) homogeneous ozonation; (ii) heterogeneous photocatalysis which utilizes the presence of oxygen; (iii) heterogeneous photocatalysis which utilizes the presence of ozone. It can be hypothesised that ozone competes with oxygen for the adsorption on the same sites of TiO_2. Therefore, the fractional coverage by oxygen, θ^*_{Ox}, and ozone, θ^*_{Oz}, can be expressed as follows:

$$\theta^*_{Ox} = \frac{K_{Ox} C_{Ox}}{1 + K_{Ox} C_{Ox} + K_{Oz} C_{Oz}} \quad (14)$$

$$\theta^*_{Oz} = \frac{K_{Oz} C_{Oz}}{1 + K_{Ox} C_{Ox} + K_{Oz} C_{Oz}} \quad (15)$$

where K_{Oz} is the equilibrium adsorption constant of ozone.

On this basis, the overall reaction rate of formate oxidation can be written as:

$$-\left(\frac{dC}{dt}\right)_{OV} = -\left(\frac{dC}{dt}\right)_{hom} - \left(\frac{dC}{dt}\right)_{photocatalytic,oxygen} - \left(\frac{dC}{dt}\right)_{photocatalytic,ozone} \quad (16)$$

$$-\left(\frac{dC}{dt}\right)_{OV} = k_{hom} C_{Oz} + \frac{S}{V}\left(k''_{Ox}\theta^*_{Ox}\theta + k''_{Oz}\theta^*_{Oz}\theta\right) = k_{hom} C_{Oz} + \frac{S}{V}\left(k''_{Ox}\theta^*_{Ox} + k''_{Oz}\theta^*_{Oz}\right)\theta \quad (17)$$

Table 1 – Kinetic parameters calculated according to the Langmuir–Hinshelwood kinetic model.

	Photocatalysis	Integrated process $C_{Oz} = 9.86 \times 10^{-5}$ M	Integrated process $C_{Oz} = 1.05 \times 10^{-4}$ M
Second order rate constant k''_{Ox} or k''_{Oz} (mol m^{-2} s^{-1})	2.5×10^{-8}	6.86×10^{-8}	6.86×10^{-8}
Equilibrium adsorption constant of formate (K or K*) (M^{-1})	100	350	550
Equilibrium adsorption constant of oxygen (K_{Ox}) (M^{-1})	6140	6140	6140
Equilibrium adsorption constant of ozone (K_{Oz}) (M^{-1})	–	8400	8400

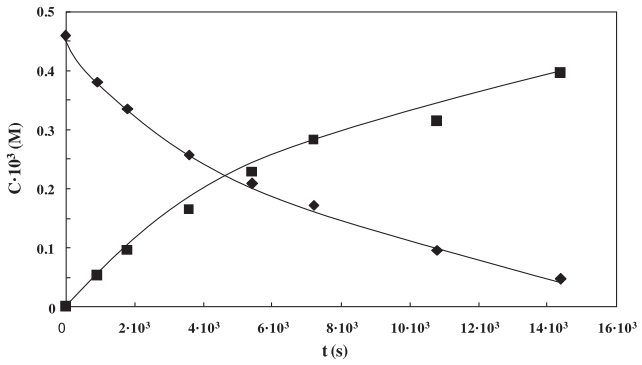

Fig. 11 – Bromate (◆) and bromide (■) concentrations versus irradiation time for a run carried out in the simultaneous presence of TiO_2, oxygen and UV-A irradiation.

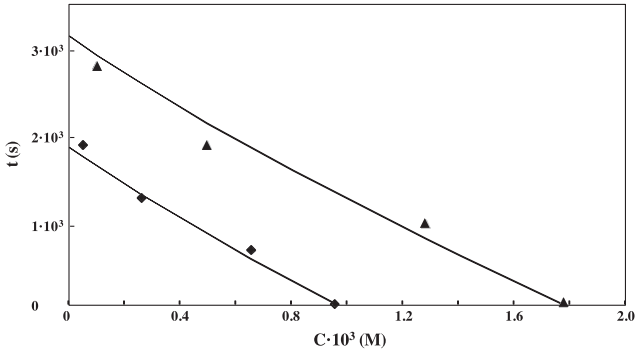

Fig. 13 – Comparison between the experimental data and the Langmuir–Hinshelwood model for selected runs of the integrated process (C_{Oz} = 1.05 × 10^{-4} M).

where the homogeneous reaction rate is zero order with respect to formate ion, k''_{Oz} is the second-order kinetic constant of the photocatalytic reaction between adsorbed ozone and formate ion and θ the fractional site coverage by formate ion when also ozone is present in the solution. By considering that ozone and oxygen concentrations can be considered constant, Eq. (17) can be simplified by substituting the $(S/V)(k''_{Ox}\theta^*_{Ox} + k''_{Oz}\theta^*_{Oz})$ term with k'_{Oz}, so that it may be written as:

$$-\left(\frac{dC}{dt}\right)_{OV} = k_{hom}C_{Oz} + k'_{Oz}\theta = k_{hom}C_{Oz} + k'_{Oz}\frac{K^*C}{1+K^*C} \quad (18)$$

where K^* is the equilibrium adsorption constant of formate ion when ozone is dissolved in the reacting medium.

Eq. 18 can be rearranged as:

$$-\left(\frac{dC}{dt}\right)_{OV} = \frac{K^*C(k_{hom}C_{Oz} + k'_{Oz}) + k_{hom}C_{Oz}}{1+K^*C} \quad (19)$$

The integration of Eq. (19) under the initial condition that at $t = 0$ the formate concentration is C_0 gives

$$t = \frac{1}{A^2K^*}\left[(A - r_{hom})\ln\frac{AK^*C_0 + r_{hom}}{AK^*C + r_{hom}} + AK^*(C_0 - C)\right] \quad (20)$$

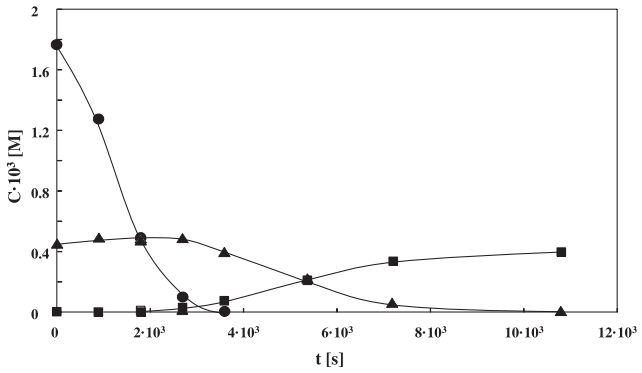

Fig. 12 – Experimental values of formate (●), bromide (▲) and bromate (■) ion concentrations vs. reaction time for a run carried out in the presence of TiO_2 (0.2 g L^{-1}), ozone (1.05 × 10^{-5} M) and UV-A irradiation: initial formate concentration 1.8 mM.

where $r_{hom} = k_{hom}\,C_{oz}$, $A = r_{homo} + k'_{Oz}$. By applying a least-squares best fitting procedure to the two sets of photoreactivity runs carried out with different ozone concentrations, the values of the k'_{Oz} and K^* terms have been obtained; the K^* values are reported in Table 1. It must be noted that the concentration of dissolved ozone does not only affect the figures of $k'_{Oz} = (k''_{Ox}\theta^*_{Ox}\theta^* + k''_{Oz}\theta^*_{Oz}\theta^*)$, but also the values of the equilibrium adsorption constant of formate anion. This unexpected outcome is in agreement with the results of other studies (Addamo et al., 2005) where oxalate ion was used instead of formate ion. From the definition of k'_{Oz} and the previously obtained values k''_{Ox} and K_{Ox}, the values of k''_{Oz} and K_{Oz} have been determined (see Table 1).

Fig. 13 shows the comparison between the experimental data and the model. Also in this case a satisfactory fit of the model to the experimental data is apparent.

Fig. 14 shows the performances obtained by the homogeneous ozonation, the photocatalysis with only oxygen and the integrated process for the degradation of formate. It can be observed that in the integrated process the formate degradation is largely faster than in both the homogeneous ozonation and in the photocatalysis with only oxygen. In fact, it is well known (Tanaka et al., 1996; Klare et al., 1999; Piera et al., 2000; Sanchez et al., 1998; Villaseñor et al., 2002; Wang et al., 2002; Hernandez-Alonso et al., 2002; Addamo et al., 2005) that a synergy occurs so that the oxidation rate in the integrated

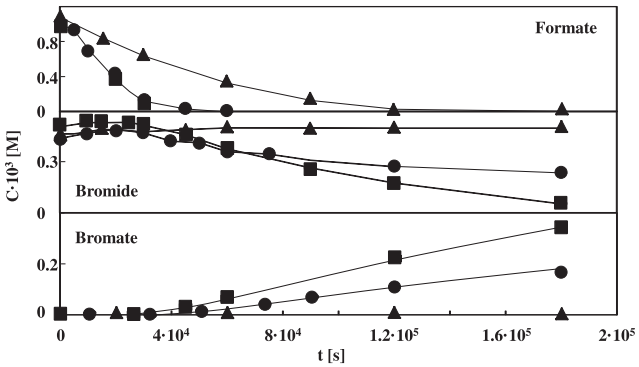

Fig. 14 – Comparison between homogeneous ozonation (●), photocatalysis without ozone (▲) and integrated process, i.e. photocatalysis with ozone (■).

process becomes higher than the sum of the rates with the sole ozonation plus the one of photocatalysis without ozone. For instance, in the present investigation the following values have been obtained for the oxidation rate of formate (initial concentration 0.5 mM): 3.83×10^{-8} M s^{-1} for only photocatalysis with oxygen and 0.01 g L^{-1} of P25-TiO_2; 2.4×10^{-7} M s^{-1} for the homogeneous ozonation in the presence of ozone (Coz = 1.05×10^{-4} M); 4.33×10^{-7} M s^{-1} for the photocatalysis in the presence of ozone and 0.01 g L^{-1} P25-TiO_2. Therefore, the sum of the oxidation rates for the photocatalysis plus the homogeneous ozonation (2.78×10^{-7} M s^{-1}) is less than 4.33×10^{-7} M s^{-1}, which is the rate with the integrated process. In the integrated process, if bromide is initially present, the concentration of the undesired bromate at the end of the run is the highest one with respect to the single processes, but its concentration remains negligible as long as the organic is not almost completely disappeared. This outcome demonstrates that bromate formation can be avoided simply by interrupting the ozonation when the oxidation of the organics is near to be completed. On the other hand, the bromate reduction is also a viable method to control its accumulation. It has been previously shown that photocatalysis is able to reduce bromate to bromide ions. Furthermore, it was also observed that the reduction rate can be enhanced in the presence of organics and it is favoured at relatively low pHs, preferably below the pH of zero point charge of the photocatalyst.

4-nitrophenol was utilized as probe molecule in substitution of the formate ion, to check the effect of the chemical nature of the contaminant. By comparing these results with those obtained using formate as the contaminant, it was found that all the behaviours remain qualitatively the same. The highest degradation rate of 4-nitrophenol is obtained with the integrated process, but in this system the formation of bromate, which again takes place only after the disappearance of 4-nitrophenol, is faster than with formate ion. As it happened with formate ions, also with 4-nitrophenol, photocatalysis without ozone degrades the organic compound without the undesired oxidation of bromide ions into hazardous bromate.

4. Conclusions

Ozonation, heterogeneous photocatalysis and their integration were studied for the oxidation of a model organic compound in aqueous solutions containing also bromide ions. The integrated process is particularly effective for water detoxification since the oxidation rate of organic compound is substantially increased with respect to the sum of the rates obtainable with the two processes acting in series.

On the contrary, when photocatalysis takes place in the presence of oxygen without ozone, the formation of bromate is inhibited. Furthermore, for this latter process the photogenerated electrons are able to reduce the possibly present bromate to bromide ions. It has been observed that, for the ozonation and the integrated process, the formation of bromate is avoided as long as the organic has not almost completely vanished. Moreover, during the photocatalytic experiments, if the pH is not too high, the presence of organics favours also the reduction of bromate into bromide regardless if ozone is present or not. On the contrary the homogeneous ozonation inhibits the reduction of bromate even in the presence of organics.

The Langmuir–Hinshelwood kinetic model adequately describes the behaviour of the heterogeneous system and it has been possible to obtain the values of the kinetic constant and of the equilibrium adsorption constant. The kinetic constant of the photocatalytic reaction in presence of ozone is higher than that obtained without ozone. Moreover, the value of the adsorption constant of formate anion increases with the ozone concentration.

It can be noted that the results obtained in the present work have relevance for practical application of these oxidation processes.

Acknowledgements

The authors FP VL GP and VA wish to thank MIUR (Rome) for economical Support (Project: PON02_00153_2849085).

REFERENCES

Addamo, M., Augugliaro, V., García-López, E., Loddo, V., Marcı', G., Palmisano, L., 2005. Oxidation of oxalate ion in aqueous suspensions of TiO_2 by photocatalysis and ozonation. Catal. Today 107–108, 612–618.

Akpan, U.G., Hameed, B.H., 2010. The advancements in sol-gel method of doped-TiO_2 photocatalysts. Appl. Catal. A: General 375, 1–11.

Akpan, U.G., Hameed, B.H., 2011(a). Solar degradation of an azo dye, acid red 1, by Ca-Ce-WTiO_2 composite catalyst. Chem. Eng. J. 169, 91–99.

Akpan, U.G., Hameed, B.H., 2011(b). Photocatalytic degradation of 2,4-dichlorophenoxyacetic acid by Ca-Ce-W-TiO_2 composite photocatalyst. Chem. Eng. J. 173, 369–375.

Ali, A.H., Kapoor, S., Kansal, S.K., 2011. Studies on the photocatalytic decolorization of pararosaniline chloride dye and its simulated dyebath effluent. Desal. Water Treat. 25, 268–275.

Amy, G., Siddiqui, M., Zhai, W., Debroux, J., Odem, W., 1994. Survey on Bromide in Drinking Water and Impacts on DBP Formation (AWWARF report, Denver, CO).

Augugliaro, V., Bianco-Prevot, A., Cáceres-Vázquez, J., García-López, E., Loddo, V., Malato-Rodríguez, S., Marcì, G., Palmisano, L., Pramauro, E., 2004. Photocatalytic oxidation of acetonitrile in aqueous suspension of titanium dioxide irradiated by sunlight. Adv. Environ. Res. 8, 329–335.

Augugliaro, V., Kisch, H., Loddo, V., Lopez-Munoz, M.J., Marquez-Alvarez, C., Palmisano, G., Palmisano, L., Parrino, F., Yurdakal, S., 2008. Photocatalytic oxidation of aromatic alcohols to aldehydes in aqueous suspension of home-prepared titanium dioxide 1. Selectivity enhancement by aliphatic alcohols. Appl. Catal. A: General 349, 182–188.

Augugliaro, V., Loddo, V., Pagliaro, M., Palmisano, G., Palmisano, L., 2010. Clean by Light Irradiation: Practical Applications of Supported TiO_2. RSC Publishing, Cambridge (UK), ISBN 978-1-84755-870-1.

Augustina, T.E., Ang, H.M., Vareek, V.K., 2005. A review of synergistic effect of photocatalysis and ozonation on

wastewater treatment. J. Photochem. Photobiol. C: Photochem. Rev. 6, 264–273.
Beltran, F.J., 2003. Ozone-UV radiation-hydrogen peroxide oxidation technologies. In: Tarr, M.A. (Ed.), Chemical Degradation Methods for Wastes and Pollutants: Environmental and Industrial Applications. Marcel Dekker Inc., New York, NY, pp. 1–75.
Bowen, H.J.M., 1979. Environmental Chemistry of the Elements. Academic Press, London.
Brookman, R.M., Lamsal, R., Gagnon, G.A., 2011. Comparing the formation of bromate and bromoform due to ozonation and UV-TiO_2 oxidation in seawater. J. Adv. Oxi. Technol. 14 (1), 23–30.
Buttler, R., Godley, A., Lytton, L., Cartmell, E., 2005. Bromate environmental contamination: review of impact and possible treatment. Crit. Rev. Environ. Sci. Technol. 35, 193–217.
Cavanagh, J.E., Weinberg, H.S., Gold, A., Sangalah, R., Marbury, D., Glaze, W.H., Collette, T.W., Richardson, S.D., Thruston Jr., A.D., 1992. Ozonation byproducts: Identification of bromohydrins from the ozonation of natural waters with enhanced bromide levels. Environ. Sci. Technol. 26, 1658–1662.
Chong, M.N., Jin, B., Chow, C.W.K., Saint, C., 2010. Recent developments in photocatalytic water treatment technology: a review. Water Res. 44, 2997–3027.
Council Directive 98/83/EC of 3 November 1998 on the quality of water intended for human consumption. OJ L 330, 5.12.1998, p. 32–54
Flury, M., Papritz, A., 1993. Bromide in the natural environment: occurrence and toxicity. J. Environ. Qual. 22, 747–758.
Forni, L., Bahnemann, D., Hart, E.J., 1982. Mechanism of hydroxide ion initiated decomposition of ozone in aqueous solution. J. Phys. Chem. 86, 255–259.
Gillogly, T., Najm, I., Watson, M., Minear, R., Marinas, B., Urban, M., Kim, J.H., Echigo, S., Amy, G., Douville, C., Daw, B., Andrews, R., Hofmann, R., Croue, J.P., 2001. Bromate Formation and Control During Ozonation of low Bromide Waters. Awwa Research Foundation American Water Works Association.
Haag, W.R., Hoigne, J., 1983. Ozonation of bromide-containing waters: kinetics of formation of hypobromous acid and bromate. Environ. Sci. Technol. 17, 261–267.
Herrmann, J.-M., 2005. Heterogeneous photocatalysis: state of the art and present applications. Topics Catal. 34, 49–65.
Hernandez-Alonso, M.D., Coronado, J.J., Maira, A.J., Soria, J., Loddo, V., Augugliaro, V., 2002. Ozone enhanced activity of aqueous titanium dioxide suspensions for photocatalytic oxidation of free cyanide ions. Appl. Catal. B: Environ. 39, 257.
Hoignè, J., 1998. Chemistry of aqueous ozone and transformation of pollutants by ozonation and advanced oxidation processes. Quality and treatment of drinking water. Handbook Environ. Chem. 5/5C, 83–141.
Hoigné, J., Bader, H., 1983. Rate constants of reactions of ozone with organic and inorganic compounds in water. II–Dissociating organic compounds. Water Res. 17, 185–194.
Hutchinson, T.H., Hutchings, M.J., Moore, K.W., 1997. A review of the effects of bromate on aquatic organisms and toxicity of bromate to oyster (Crassostrea Gigas) embryos. Ecotoxicol. Environ. Saf. 38, 238–243.
Ibhadon, A.O., Fitzpatrick, P., 2013. Heterogeneous photocatalysis: recent advances and applications. Catalysts 3, 189–218.
Kittel, H., 1983. Substances Usable in Substitution of 2-nitropropane and 1,2 Dibromoethane (Ersatzstoffe für 2-nitropropan und 1,2 dibromoethan). Schriftenreihe Gefährliche Arbeitsstoffe No. 11. Dortmund. Wirtschaftsverlag NW, Bremerhaven.
Klare, M., Waldner, G., Bauer, R., Jacobs, H., Broekaert, J.A.C., 1999. Degradation of nitrogen containing organic compounds by combined photocatalysis and ozonation. Chemosphere 38 (9), 2013–2027.
Krasner, S.W., McGuire, M.J., Jacangelo, J.G., Patania, N.L., Reagan, K.M., Aieta, E.M., 1989. Occurrence of DBPs in US drinking water. J. Am. Water Works Assoc. 81, 41–53.
Lide, D.R. (Ed.), 1994. Handbook of Chemistry and Physics. CRC Press Inc., Boca Raton.
Mas, D., Pichat, P., Guillard, C., Luck, F., 2005. Removal of monochloroacetic acid in water by advanced oxidation based on ozonation in the presence of TiO_2 irradiated at λ>340 nm. Ozone: Sci. Eng. 27, 311–316.
Muneer, M., Qamar, M., Saquib, M., Bahnemann, D., 2005. Heterogeneous photocatalysed reaction of three selected pesticide derivatives, propham, propachlor and tebuthiuron in aqueous suspension of titanium dioxide. Chemosphere 61, 457–468.
Nawrocki, J., Kasprzyk-Hordern, B., 2010. The efficiency and mechanisms of catalytic ozonation. Appl. Catal. B: Environ. 99, 27–42.
Neal, C., Neal, M., Hughes, S., Wickham, H., Hill, L., Harman, S., 2007. Bromine and bromide in rainfall, cloud, stream and groundwater in the Plynlimon area of mid-Wales. Hydrol. Earth Syst. Sci. 11 (1), 301–312.
Ohtani, B., Zhang, S.-W., Nishimoto, S.-I., Kagiya, T., 1992. Catalytic and photocatalytic decomposition of ozone at room temperature over titanium(IV) oxide. J. Chem. Soc. Faraday Transact. 88, 1049–1053.
Pichat, P., Disdier, J., Hoang-Van, C., Mas, D., Goutailler, G., Gaysse, C., 2000. Purification/deodorization of indoor air and gaseous effluents by TiO_2 photocatalysis. Catal. Today 63, 363–369.
Pichat, P. (Ed.), 2013. Photocatalysis and Water Purification. From Fundamentals to Applications. Wiley-VCH, Weinheim.
Piera, E., Calpe, J.C., Brillas, E., Doménech, X., Peral, J., 2000. 2,4-Dichlorophenoxyacetic acid degradation by catalyzed ozonation: TiO2/UVA/O3 and Fe(II)/UVA/O3 systems. Appl. Catal. B: Environ. 27 (3), 169–177.
Ravelli, D., Dondi, D., Fagnonia, M., Albini, A., 2009. Photocatalysis. A multi-faceted concept for green chemistry. Chem. Soc. Rev. 38, 1999–2011.
Richardson, S.D., Thruston Jr., A.D., Caughran, T.V., Chen, P.H., Collette, T.W., Floyd, T.L., Schenck, K.M., Lykins Jr., B.W., Sun, G., Majetich, G., 1999. Identification of new ozone disinfection byproducts in drinking water. Environ. Sci. Technol. 33, 3378–3383.
Sanchez, L., Peral, J., Domenech, X., 1998. Aniline degradation by combined photocatalysis and ozonation. Appl. Catal. B: Environ. 19, 59–65.
Siddiqui, M., Amy, G., Rice, R., 1995. Bromate ion formation: a critical review. J. Am. Water Works Assoc. 87, 58–70.
Song, R., Minear, R., Westerhoff, P., Amy, G., 1996. Modelling and risk analysis of bromate formation from ozonation of bromide-containing waters. Water Sci. Technol. 34, 79–85.
Staehelin, J., Hoigné, J., 1982. Decomposition of ozone in water: rate of initiation by hydroxide ions and hydrogen peroxide. Environ. Sci. Technol. 16, 676–681.
Staehelin, J., Hoigné, J., 1985. Decomposition of ozone in water in the presence of organic solutes acting as promoters and inhibitors of radical chain reactions. Environ. Sci. Technol. 19, 1206–1213.
Sunada, K., Watanabe, T., Hashimoto, K., 2003. Studies on photokilling of bacteria on TiO_2 thin film. J. Photochem. Photobiol. A: Chem. 156, 227–233.
Tanaka, K., Abe, K., Hisanaga, T., 1996. Photocatalytic water treatment on immobilized TiO_2 combined with ozonation. J. Photochem. Photobiol. A 101, 85–87.
Taranto, J., Frochot, D., Pichat, P., 2007. Combining cold plasma and TiO_2 photocatalysis to purify gaseous effluents: a

preliminary study using methanol-contaminated air. Ind. Eng. Chem. Res. 46, 7611–7614.
Villaseñor, J., Reyes, P., Pecchi, G., 2002. Catalytic and photocatalytic ozonation of phenol on MnO_2 supported catalysts. Catal. Today 76 (2), 121–131.
Von Gunten, U., 2003. Ozonation of drinking water: Part I. Oxidation kinetics and product formation. Water Res. 37, 1443–1467.
Von Gunten, U., Pinkernell, U., 2000. Ozonation of bromide-containing drinking waters: a delicate balance between disinfection and bromate formation. Water Sci. Technol. 41, 53–59.
Wang, S., Shiraishi, F., Nakano, K., 2002. A synergistic effect of photocatalysis and ozonation on decomposition of formic acid in an aqueous solution. Chem. Eng. J. 87, 261–271.
World Health Organization, 1993. Guidelines for Drinking Water Quality. WHO, Geneva, Switzerland.
Yapsakli, K., Can, Z.S., 2004. Interaction of ozone with formic acid: a system which suppresses the scavenging effect of HCO_3^-/CO_3^{2-}. Water Qual. Res. J. Canada 39, 140–148.
Yuita, K., 1983. Iodine, bromine and chlorine contents in soils and plants of Japan. Soil Sci. Plant Nutr. 29, 403–428.